

P.2024

## A uniform strain, discrete-grain model for evolving anisotropy of polycrystalline ice

R. STAROSZCZYK<sup>1)</sup>

*School of Mathematics, University of East Anglia  
Norwich NR4 7TJ, United Kingdom  
e-mail : r.staroszczyk@uea.ac.uk*

A DISCRETE-GRAIN MODEL accounting for the induced anisotropy of polycrystalline ice is formulated. An individual ice crystal is supposed to be a transversely isotropic medium whose behaviour is linearly viscous. For such a crystal a frame-indifferent constitutive law involving three microscopic rheological parameters is derived. Assuming that each crystal undergoes a homogeneous deformation of the polycrystalline aggregate (the Taylor approximation), the macroscopic viscous behaviour of the material is determined. The considerations are illustrated by the results of numerical simulations of simple flows, showing the evolution of the oriented structure of the material and the variation of macroscopic viscosities with increasing strains. In addition, the influence of the parameters describing the single crystal anisotropy on the overall behaviour of the aggregate is investigated.

**Key words:** polycrystalline ice, induced anisotropy, constitutive law.

### Notations

$A, B$	ice crystal dimensionless rheological parameters
$c$	crystal $c$ -axis unit vector
$D$	strain-rate tensor
$I$	unit tensor
$L$	velocity gradient tensor
$M$	structural tensor
$Q$	rotation matrix
$S$	deviatoric Cauchy stress tensor
$W$	spin tensor
$x_i$ ( $i = 1, 2, 3$ )	global spatial Cartesian co-ordinates
$x_i^g$ ( $i = 1, 2, 3$ )	local spatial Cartesian co-ordinates
$\vartheta$	angle defining the crystal $c$ -axis orientation
$\kappa$	shear strain
$\mu$	viscosity for shear on a crystal basal plane
$\mu_0$	isotropic polycrystalline ice viscosity
$\mu_{ij}$ ( $i, j = 1, 2, 3$ )	instantaneous viscosities
$\sigma$	Cauchy stress tensor
$\varphi$	angle defining the crystal $c$ -axis orientation

<sup>1)</sup>On leave from the Institute of Hydroengineering, Polish Academy of Sciences, ul. Waryńskiego 17, 71-310 Szczecin, Poland

## 1. Introduction

ICE CORES RETRIEVED from polar ice caps in Antarctica and Greenland reveal strong fabrics (THORSTEINSSON *et al.* [31]), with individual ice grain *c*-axes (the axes of the crystal hexagonal symmetry) aligned along some preferential directions, with the degree of the alignment usually increasing with the depth of ice, in response to changing loading conditions. Such a phenomenon, in which the internal structure of the material, and hence its macroscopic properties, evolve due to current stress and strain configurations, is known as induced anisotropy.

The main mechanisms taking place on the microscopic level of a single ice grain that are involved in the formation and subsequent evolution of the oriented structure of the medium include, according to ALLEY [1], (1) crystal lattice rotation, a process, in which the crystal *c*-axes rotate towards the principal axes of compression and away from the principal axes of extension, (2) polygonisation (also referred to as rotation recrystallisation), a mechanism in which the existing crystals are split and new grains are formed, and (3) dynamic (or migration) recrystallisation, a process phenomenon in which, due to high shear stresses and high temperatures, new grains are created at the expense of old grains that subsequently disappear. The role of these three micro-processes changes considerably with the depth in an ice sheet. In the present work, we are concerned with only the first of these processes, namely the crystal lattice rotation, a mechanism which, unlike the other two, occurs throughout the whole depth of a polar ice cap, and dominates the evolution of ice fabric in the upper half of a polar ice sheet.

A single crystal of ice is highly anisotropic, much more anisotropic than most metallic crystals. As indicated by DUVAL *et al.* [9], a stress needed to shear the crystal on its basal plane at a given strain-rate is about two orders of magnitude smaller than those required for other, non-basal, slips. The hexagonal symmetry of the ice monocrystal is practically insignificant in terms of its mechanical behaviour, therefore the single grain can be regarded as a transversely isotropic body (KAMB [16]). At temperatures and stresses typical of polar ice masses, ice deforms mainly by viscous creep. Plastic (rate-independent) behaviour is observed only at the stress magnitudes of 100 MPa (DUVAL *et al.* [9]), by far exceeding those occurring in natural conditions. The strong anisotropy of the single crystal has significant consequences for the overall flow of polar ice sheets as the oriented structure of the polycrystalline material develops. This has been confirmed by the results of numerical simulations of polar ice sheets (MANGENEY *et al.* [19, 20], STAROSZCZYK and MORLAND [29]), showing that the rates at which the whole sheet flows are about twice as high for an anisotropic ice with oriented fabric than those calculated on the assumption of isotropic ice with a random distribution of crystal *c*-axes. This clearly indicates that the mechanism



of induced anisotropy must be taken into account in the analysis of polar ice behaviour if realistic results are to be obtained.

When modelling the behaviour of polycrystalline ice, a material with evolving micro-structure, two distinct approaches can be pursued. In the first approach, based on the methods of classical continuum mechanics, ice is treated as a continuum in which each material point contains crystals of all possible orientations. The distribution of these orientations in space can be described by a so-called orientation distribution function, whose evolution determines the directional changes in the internal structure of the aggregate (SVENDSEN and HUTTER [30], MEYSSONNIER and PHILIP [21], GÖDERT and HUTTER [14], GAGLIARDINI and MEYSSONNIER [21], GAGLIARDINI *et al.* [11]). Another continuum approach, in which the micro-structure of ice is ignored by assuming that the macroscopic behaviour of the material depends entirely on the macroscopic variables, such as stress, strain-rate and strain, has been followed by MORLAND and STAROSZCZYK [24], STAROSZCZYK and MORLAND [28] and STAROSZCZYK [26].

A fundamentally different approach is to treat each point of the polycrystal as a collection of a finite number of discrete grains. In such a method the behaviour of each crystal is followed separately, and the macroscopic response of ice is derived from the responses of all individual grains by applying a homogenisation technique. Employing this method, AZUMA [2] has developed a model, in which an individual crystal is assumed to deform only by basal slip, and the microscopic stress applied to each crystal is related to the bulk macroscopic stress in a way determined on the basis of experimental results. VAN DER VEEN and WHILLANS [32] have adopted a similar approach, by supposing that the only slip system active during the viscous deformation of a grain is that associated with basal gliding, but, following LLIBOUTRY [17], have made an assumption of a uniform stress, requiring that the stress in each grain is the same as the macroscopic stress applied to the polycrystal. Yet another approach is the self-consistent model based on the theory developed by HUTCHINSON [15] and extended by MOLINARI *et al.* [23], in which no assumptions on the relations between the microscopic and macroscopic strains and stresses are needed. In that formulation each crystal is treated as an idealised geometric inclusion in an infinite homogeneous medium with properties supposed to represent the macroscopic behaviour of the polycrystal, and on this basis interaction forces between the grain and the aggregate are determined. Following this method, CASTELNAU *et al.* [7] have constructed a model for polycrystalline ice in which the crystal slips on basal, prismatic and pyramidal planes are incorporated.

In this work we formulate a discrete-grain model, in which the crystal slips can occur on basal and prismatic planes (the latter are the planes parallel to the crystal *c*-axis), which in terms of its generality and complexity places this model between the simpler AZUMA [2] and VAN DER VEEN and WHILLANS [32] models

on one side, and the much more complex and elaborate CASTELNAU *et al.* [7] model on the other. A single crystal is supposed to be a transversely isotropic and linearly viscous medium. The anisotropic properties of the crystal are described by means of two rheological parameters. For such a material, a constitutive law that relates microscopic stresses to strain-rates is formulated. Adopting then the Taylor assumption of the homogeneity of strain throughout the polycrystalline aggregate, a uniform deformation model is constructed. Correlating the model predictions with experimental data describing the limit macroscopic viscosities of ice in compression and simple shear, the two microscopic rheological parameters are determined. For illustration purposes, the model is used to simulate the viscous behaviour of polycrystalline ice in uniaxial compression and simple shear flows. The results obtained demonstrate how the initially isotropic fabric with a random distribution of crystal *c*-axes evolves as the deformation proceeds, and the variation of the macroscopic viscosities with increasing deformation is illustrated. In addition, the influence of the two rheological parameters describing the anisotropy of the single grain on the macroscopic behaviour of a polycrystalline ice aggregate is investigated.

## 2. Single crystal kinematics

We adopt material rectangular Cartesian co-ordinates  $OX_i$  ( $i = 1, 2, 3$ ) with base vectors  $\mathbf{e}_i$  ( $i = 1, 2, 3$ ), and fixed spatial rectangular co-ordinates  $Ox_i$  ( $i = 1, 2, 3$ ) with the same origin  $O$  and the base vectors  $\mathbf{e}_i$ . In order to describe a changing position of a single crystal, we use a local spatial reference frame associated with the ice grain, with the axes  $Ox_i^g$  ( $i = 1, 2, 3$ ) and the base vectors  $\mathbf{e}_i^g$ .

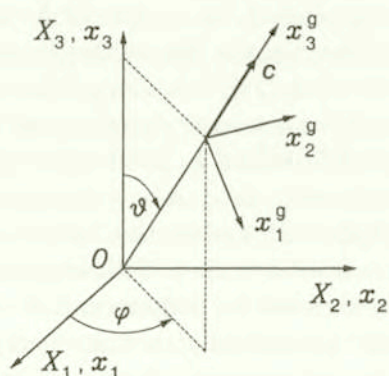


FIG. 1. Global and local co-ordinate systems, with the angles  $\theta$  and  $\varphi$  defining the crystal *c*-axis orientation.



Due to the transverse isotropy of the single crystal of ice, with the direction of the axis of its transverse symmetry coinciding with the crystal  $c$ -axis and defined by the unit vector  $\mathbf{c}$ , it suffices to follow the orientation of the vector  $\mathbf{c}$  in space to uniquely describe the position of an individual crystal. Accordingly, we assume that  $\mathbf{c} = \mathbf{e}_3^g$ , and to complete the definition of the local reference frame, we further assume that the  $x_1^g$  axis lies in the meridian plane  $Ox_3x_3^g$ , and the  $x_2^g$  axis is chosen in such a way that the right-handedness of the local co-ordinate system is preserved (see Fig. 1).

In order to position the local frame  $Ox_i^g$  relative to the global frame  $Ox_i$ , we introduce two angles: the co-latitude, or the zenith angle,  $\vartheta$ , and the longitude  $\varphi$ . In terms of these two angles, the rotation matrix  $\mathbf{Q}$ , with the components given by  $Q_{ij} = \mathbf{e}_i \cdot \mathbf{e}_j^g$ , which transforms the components of non-scalar quantities from the local to the global reference frame, is given by

$$(2.1) \quad \mathbf{Q} = \begin{pmatrix} \cos \vartheta \cos \varphi & -\sin \varphi & \sin \vartheta \cos \varphi \\ \cos \vartheta \sin \varphi & \cos \varphi & \sin \vartheta \sin \varphi \\ -\sin \vartheta & 0 & \cos \vartheta \end{pmatrix}.$$

In what follows, we will be concerned with both microscopic quantities, referring to the behaviour of an individual crystal of ice, and macroscopic quantities, describing the behaviour of a polycrystalline aggregate as a whole; the latter quantities will be indicated by a superposed bar. Further, the components of tensor entities expressed in the local reference frame will be denoted by the superscript  $g$ , while those expressed in the global reference frame will be left without any suffix. Thus,  $\mathbf{A}^g$  indicates a microscopic tensor quantity whose components are expressed in the co-ordinate system  $Ox_i^g$  associated with a single grain, while  $\bar{\mathbf{A}}$  denotes a macroscopic tensor quantity whose components are expressed in the global co-ordinate system  $Ox_i$ , etc.

Since in the problem at hand the internal structure of the material evolves, which is due to the change in time of the crystal  $c$ -axes orientations in space, the local frames  $Ox_i^g$  ( $i = 1, 2, 3$ ) associated with individual grains of ice rotate relative to the fixed global frame  $Ox_i$  ( $i = 1, 2, 3$ ) as the deformation of the polycrystalline aggregate occurs. Therefore, the matrix  $\mathbf{Q}$  which describes the transformation of tensor entities between the frames  $Ox_i$  and  $Ox_i^g$  is time-dependent, that is  $\mathbf{Q} = \mathbf{Q}(t)$ . Hence, the relations connecting the global and local position vectors,  $\mathbf{x}$  and  $\mathbf{x}^g$  respectively, have the following forms:

$$(2.2) \quad \mathbf{x} = \mathbf{Q}(t)\mathbf{x}^g, \quad \mathbf{x}^g = \mathbf{Q}^T(t)\mathbf{x}, \quad \mathbf{x} = \mathbf{x}(\mathbf{X}, t), \quad \mathbf{x}^g = \mathbf{x}^g(\mathbf{X}, t),$$

with the vector  $\mathbf{X}$  containing the material co-ordinates, common for both reference systems  $Ox_i$  and  $Ox_i^g$ ,  $\mathbf{Q}^T$  being the transpose of  $\mathbf{Q}$ , and  $t$  denoting time.

Differentiation with respect to time of the relations describing the properties of orthogonal matrices

$$(2.3) \quad \mathbf{Q}\mathbf{Q}^T = \mathbf{Q}^T\mathbf{Q} = \mathbf{I},$$

where  $\mathbf{I}$  is the unit tensor, yields the relations

$$(2.4) \quad \dot{\mathbf{Q}}\mathbf{Q}^T + \mathbf{Q}\dot{\mathbf{Q}}^T = \mathbf{O}, \quad \dot{\mathbf{Q}}^T\mathbf{Q} + \mathbf{Q}^T\dot{\mathbf{Q}} = \mathbf{O},$$

in which superposed dots denote time derivatives. In view of (2.2)<sub>1</sub>, the velocity fields observed in the global and local frames,  $\mathbf{v}$  and  $\mathbf{v}^g$  respectively, are related by

$$(2.5) \quad \mathbf{v} = \dot{\mathbf{x}} = \dot{\mathbf{Q}}\mathbf{x}^g + \mathbf{Q}\dot{\mathbf{x}}^g = \dot{\mathbf{Q}}\mathbf{x}^g + \mathbf{Q}\mathbf{v}^g.$$

By differentiating (2.5) and (2.2)<sub>2</sub> with respect to the spatial co-ordinates  $x_i$  ( $i = 1, 2, 3$ ), we obtain the following equation that connects the velocity gradient tensors  $\mathbf{L}$  and  $\mathbf{L}^g$  (whose components are  $L_{ij} = \partial v_i / \partial x_j$  and  $L_{ij}^g = \partial v_i^g / \partial x_j^g$ , respectively), measured in the global and local co-ordinate systems:

$$(2.6) \quad \mathbf{L} = \dot{\mathbf{Q}}\mathbf{Q}^T + \mathbf{Q}\mathbf{L}^g\mathbf{Q}^T.$$

The relations (2.6) and (2.4) provide the transformation formulae for the strain-rate and spin tensors. The strain-rate tensors  $\mathbf{D}$  and  $\mathbf{D}^g$ , the symmetric parts of  $\mathbf{L}$  and  $\mathbf{L}^g$ , respectively, are related by

$$(2.7) \quad \mathbf{D} = \mathbf{Q}\mathbf{D}^g\mathbf{Q}^T,$$

while the spin tensors  $\mathbf{W}$  and  $\mathbf{W}^g$ , the anti-symmetric parts of  $\mathbf{L}$  and  $\mathbf{L}^g$ , respectively, are connected by

$$(2.8) \quad \mathbf{W} = \dot{\mathbf{Q}}\mathbf{Q}^T + \mathbf{Q}\mathbf{W}^g\mathbf{Q}^T.$$

The presence of the term  $\dot{\mathbf{Q}}\mathbf{Q}^T$  in Eq. (2.8) reflects the fact that the angular velocity in the global system  $Ox_i$  is the vector sum of the angular velocity in the local system  $Ox_i^g$  and the angular velocity of  $Ox_i^g$  with respect to  $Ox_i$ . As the spin tensor  $\mathbf{W}$  is a skew-symmetric tensor, it follows that the matrix equation (2.8) is equivalent to the set of three independent differential equations. Since the matrix  $\mathbf{Q}(t)$ , which defines the orientation of the crystal  $c$ -axis, and hence the ice fabric, is a function of two variables, the angles  $\vartheta$  and  $\varphi$ , we need to prescribe altogether five (out of six) independent components of the spin tensors  $\mathbf{W}$  and  $\mathbf{W}^g$  in order to determine the rotation of an individual crystal.



Now, by equating, in turn, the components  $(\ )_{12}$ ,  $(\ )_{13}$ , and  $(\ )_{23}$  in (2.8), and using the definition (2.1) of the matrix  $\mathbf{Q}$ , we obtain the following three relations describing the evolution of the grain orientation:

$$(2.9) \quad \dot{\varphi} \cos \vartheta = W_{12}^g - W_{12} \cos \vartheta + (W_{13} \sin \varphi - W_{23} \cos \varphi) \sin \vartheta,$$

$$(2.10) \quad \dot{\vartheta} = -W_{13}^g + W_{13} \cos \varphi + W_{23} \sin \varphi,$$

$$(2.11) \quad \dot{\varphi} \sin \vartheta = -W_{23}^g - W_{12} \sin \vartheta - (W_{13} \sin \varphi - W_{23} \cos \varphi) \cos \vartheta.$$

From among five independent components of the microscopic spin tensors  $\mathbf{W}$  and  $\mathbf{W}^g$  which need to be prescribed, three, namely those expressed in the global frame  $Ox_i$ , will be further related to the components of the macroscopic spin tensor  $\bar{\mathbf{W}}$ . Accordingly, only two components of  $\mathbf{W}^g$  must be determined on the microscopic level. This is done by following MEYSSONNIER and PHILIP [21], and assuming that the grain basal planes remain parallel to each other throughout the viscous deformation of the crystal, which implies that the velocity component in the direction of the  $c$ -axis (coinciding with the  $x_3^g$  axis) is a function of the  $x_3^g$  co-ordinate only, that is  $v_3^g = v_3^g(x_3^g)$ . Thus,  $\partial v_3^g / \partial x_1^g = \partial v_3^g / \partial x_2^g = 0$ , which results in the following two kinematic relations connecting the spin and strain-rate tensor components in the local reference frame  $Ox_i^g$ :

$$(2.12) \quad W_{13}^g = D_{13}^g, \quad W_{23}^g = D_{23}^g.$$

Hence, the only microscopic spin tensor component not yet prescribed is  $W_{12}^g$ . Its value can be determined from Eq. (2.9), given the current values of the angles  $\vartheta$  and  $\varphi$  as well as the spin tensor components in the global frame  $Ox_i$ . Since  $W_{12}^g$  describes the rotation of the crystal about its axis of symmetry measured in the local reference frame  $Ox_i^g$ , and this rotation does not affect the viscous response of the crystal due to the assumed transverse isotropy of the grain, the actual value of  $W_{12}^g$  is irrelevant to our problem. For this reason, we can ignore the relation (2.9) in our considerations, and restrict our attention to Eqs. (2.10) and (2.11) which, in view of (2.12), become

$$(2.13) \quad \dot{\vartheta} = -D_{13}^g + W_{13} \cos \varphi + W_{23} \sin \varphi,$$

$$(2.14) \quad \dot{\varphi} \sin \vartheta = -D_{23}^g - W_{12} \sin \vartheta - (W_{13} \sin \varphi - W_{23} \cos \varphi) \cos \vartheta.$$

The above two kinematic equations describe uniquely the evolution of the crystal  $c$ -axis orientation as long as the microscopic strain-rates  $D_{13}^g$  and  $D_{23}^g$  measured in the lattice frame  $Ox_i^g$  are known. In the uniform strain approach adopted here, the latter variables will be expressed in terms of the macroscopic

strain-rates, while in the uniform stress model the strain-rates  $D_{13}^g$  and  $D_{23}^g$  would be related to the macroscopic (equal to microscopic) stresses through a constitutive law for the single crystal.

### 3. Constitutive law for a single crystal of ice

It is generally accepted in theoretical glaciology that the creep behaviour of ice obeys a Norton-Hoff-type power law, stating that, in the case of uniaxial loading, the strain-rate is proportional to some power of the applied stress magnitude (GLEN [13]). At the deviatoric stresses larger than 0.2 MPa, the power law exponent  $N$  for polycrystalline ice aggregate is equal to about 3, while for a single crystal its value is  $N \sim 2$  (DUVAL *et al.* [9]). At lower stress levels, however, which are more pertinent to polar ice sheets where the deviatoric stresses are usually smaller than 0.1 MPa, both laboratory and field measurements (DOAKE and WOLFF [8], LLIBOUTRY and DUVAL [18], ALLEY [1]) give indications that the exponent  $N$  can be lower than 2, and at very low stresses possibly approaching a value close to unity. The latter flow regime corresponds to that of Harper-Dorn creep observed in many metals (LLIBOUTRY and DUVAL [18]). Such a nearly Newtonian viscous flow, with  $N \sim 1$ , seems to be a dominant material behaviour in the central, upper part of a large polar ice sheet, though a definite conclusion whether the assumption of  $N \sim 1$  at small stress levels is the best approximation to the real ice behaviour can be made only after more empirical data is available (BARAL *et al.* [3]). In this work we restrict our attention to a linear constitutive law for ice, assuming that  $N = 1$ . Nonlinearity of the creep of ice can be incorporated in the constitutive model by relating the isotropic ice viscosity to the strain-rate invariant  $\text{tr } \mathbf{D}^2$ , which is a conventional approach in glaciology.

An individual grain of ice is assumed to be a transversely isotropic material, with the crystal  $c$ -axis being the axis of the rotational symmetry. The medium is supposed to be incompressible, which is a common ice mechanics assumption, and its material behaviour is approximated by a linearly viscous flow law. Therefore, the necessary variables which the constitutive law should include are the Cauchy stress  $\boldsymbol{\sigma}$  and the strain-rate  $\mathbf{D}$ . In order to account for the transverse symmetry of the material, we introduce a structural tensor  $\mathbf{M}$  defined by

$$(3.1) \quad \mathbf{M} = \mathbf{c} \otimes \mathbf{c}, \quad M_{ij} = c_i c_j \quad (i, j = 1, 2, 3),$$

which has the property  $\text{tr } \mathbf{M} = 1$ .

Our starting point is the general theory of frame-indifferent (objective) constitutive laws (BOEHLER [5]). In accordance with this theory, the most general



linear constitutive equation for a transversely isotropic material, which relates two symmetric second-order tensors (in our case  $\sigma$  and  $\mathbf{D}$ ), has the form

$$(3.2) \quad \sigma = \alpha_1 \mathbf{I} + \alpha_2 \mathbf{M} + \alpha_3 \mathbf{D} + \alpha_4 (\mathbf{MD} + \mathbf{DM}),$$

where  $\alpha_1$  and  $\alpha_2$  are functions of the invariants  $\text{tr } \mathbf{D}$  and  $\text{tr } \mathbf{MD}$  and  $\alpha_3$  and  $\alpha_4$  are constants. The "anisotropic" invariant  $\text{tr } (\mathbf{MD}) = \mathbf{c}^T \mathbf{D} \mathbf{c}$  describes the components of  $\mathbf{D}$  in the privileged material direction represented by the vector  $\mathbf{c}$ , parallel to the crystal  $c$ -axis. The coefficients  $\alpha_k$  ( $k = 1, \dots, 4$ ) are given by

$$(3.3) \quad \begin{aligned} \alpha_1 &= a_1 + a_2 \text{tr } \mathbf{D} + a_3 \text{tr } (\mathbf{MD}), \\ \alpha_2 &= a_4 + a_5 \text{tr } \mathbf{D} + a_6 \text{tr } (\mathbf{MD}), \\ \alpha_3 &= a_7, \quad \alpha_4 = a_8, \end{aligned}$$

that is there are eight material constants ( $a_1, \dots, a_8$ ) in the most general linear law. However, the ice incompressibility condition imposes the restriction  $\text{tr } \mathbf{D} = 0$ , so the parameters  $a_2$  and  $a_5$ , providing they are of finite values, do not affect the stress response of the material and therefore can be discarded from the analysis, reducing the number of constants left for prescription to six. Further reduction of the number of constants is achieved by assuming that there exist a natural, stress-free state of the material when it does not flow, that is  $\sigma = \mathbf{O}$  when  $\mathbf{D} = \mathbf{O}$ . Hence,

$$(3.4) \quad \mathbf{D} = \mathbf{O} \Rightarrow \sigma = \alpha_1 \mathbf{I} + \alpha_2 \mathbf{M} = a_1 \mathbf{I} + a_4 \mathbf{M} = \mathbf{O},$$

as  $\alpha_1 = a_1$  and  $\alpha_2 = a_4$  when  $\mathbf{D} = \mathbf{O}$ . By multiplying both sides of (3.4) by  $\mathbf{M}$  we obtain

$$(3.5) \quad \mathbf{M}\sigma = a_1 \mathbf{M} + a_4 \mathbf{M}^2 = (a_1 + a_4) \mathbf{M} = \mathbf{O},$$

due to the identity  $\mathbf{M}^2 = \mathbf{M}$ . Calculating now the traces of the tensors entering the relations (3.4) and (3.5) we find that

$$(3.6) \quad 3a_1 + a_4 = 0 \quad \text{and} \quad a_1 + a_4 = 0,$$

resulting in  $a_1 = a_4 = 0$ , so there are only four non-vanishing constants left in the viscous flow law (3.2). Due to the ice incompressibility assumption, the mean pressure in the material is a workless constraint that is not given by a constitutive equation, therefore only the deviatoric stresses determine the creep response of ice. Hence, by equating the deviatoric parts of both sides of (3.2), we obtain the relation

$$(3.7) \quad \sigma^D = \alpha_1 \mathbf{I}^D + \alpha_2 \mathbf{M}^D + \alpha_3 \mathbf{D}^D + \alpha_4 (\mathbf{MD} + \mathbf{DM})^D,$$

where:

$$(3.8) \quad \sigma^D = \mathbf{S} = \boldsymbol{\sigma} - \frac{1}{3} \text{tr } \boldsymbol{\sigma} \mathbf{I} = \boldsymbol{\sigma} + p \mathbf{I}, \quad p = -\frac{1}{3} \text{tr } \boldsymbol{\sigma},$$

with  $\mathbf{S}$  denoting the deviatoric Cauchy stress and  $p$  being the hydrostatic pressure,  $\mathbf{I}^D = \mathbf{O}$  (as  $\mathbf{I}$  is a spherical tensor),  $\mathbf{M}^D = \mathbf{M} - \frac{1}{3} \mathbf{I}$ ,  $\mathbf{D}^D = \mathbf{D}$  (as  $\text{tr } \mathbf{D} = 0$ ), and

$$(3.9) \quad (\mathbf{MD} + \mathbf{DM})^D = \mathbf{MD} + \mathbf{DM} - \frac{2}{3} \text{tr}(\mathbf{MD}) \mathbf{I}.$$

Accordingly, Eq. (3.7) becomes

$$(3.10) \quad \mathbf{S} = \alpha_2 \mathbf{M}^D + \alpha_3 \mathbf{D} + \alpha_4 (\mathbf{MD} + \mathbf{DM})^D,$$

and we note that the coefficient  $\alpha_1 = a_3$  does no longer appear in the constitutive relation, so it now includes only three material constants:  $\alpha_2 = a_6 \text{tr}(\mathbf{MD})$ ,  $\alpha_3 = a_7$ , and  $\alpha_4 = a_8$ . Thus, the constitutive law for a single, transversely isotropic and incompressible crystal of ice can be expressed in the form:

$$(3.11) \quad \mathbf{S} = a_6 \text{tr}(\mathbf{MD}) (\mathbf{M} - \frac{1}{3} \mathbf{I}) + a_7 \mathbf{D} + a_8 \left[ \mathbf{MD} + \mathbf{DM} - \frac{2}{3} \text{tr}(\mathbf{MD}) \mathbf{I} \right].$$

The three constants  $a_6$ ,  $a_7$  and  $a_8$ , defining the viscous response of the material, should (ideally) be determined from the results of simple laboratory experiments. Assume that we are able to measure three viscosities for the single crystal, namely:  $\mu_{13}$  for shearing in the plane parallel to the crystal  $c$ -axis (so-called basal shearing),  $\mu_{12}$  for shearing in the plane normal to the  $c$ -axis (so-called prismatic shearing), and  $\mu_{33}$  for unconfined axial compression carried out along the  $c$ -axis. These three viscosities are defined in terms of the deviatoric stresses and strain-rates expressed in the local co-ordinate system  $Ox_i^g$  as follows:

$$(3.12) \quad \mu_{ij} = \frac{\mathbf{S}_{ij}^g}{2D_{ij}^g},$$

where the factor 2 appears to conform to the classical form of the flow law for viscous isotropic fluids  $\mathbf{S} = 2\mu_0 \mathbf{D}$ , with  $\mu_0$  denoting the isotropic fluid viscosity. Adopting the global reference frame  $Ox_i$  to coincide with the local frame  $Ox_i^g$  attached to the crystal, in which case  $\mathbf{S} = \mathbf{S}^g$  and  $\mathbf{D} = \mathbf{D}^g$ , the tensors and their combinations entering the relation (3.11) are given by

$$(3.13) \quad \mathbf{M} = \begin{pmatrix} 0 & 0 & 0 \\ 0 & 0 & 0 \\ 0 & 0 & 1 \end{pmatrix}, \quad \mathbf{MD}^g = \begin{pmatrix} 0 & 0 & 0 \\ 0 & 0 & 0 \\ D_{31}^g & D_{32}^g & D_{33}^g \end{pmatrix}, \quad \text{tr}(\mathbf{MD}^g) = D_{33}^g,$$



$$(3.14) \quad \mathbf{MD}^g + \mathbf{D}^g\mathbf{M} - \frac{2}{3} \operatorname{tr}(\mathbf{MD}^g)\mathbf{I} = \begin{pmatrix} -\frac{2}{3}D_{33}^g & 0 & D_{13}^g \\ 0 & -\frac{2}{3}D_{33}^g & D_{23}^g \\ D_{31}^g & D_{32}^g & \frac{4}{3}D_{33}^g \end{pmatrix}.$$

With (3.13) and (3.14), the law (3.11) provides the relations that connect the deviatoric stresses  $S_{ij}^g$  to the corresponding strain-rates  $D_{ij}^g$  by

$$(3.15) \quad S_{12}^g = a_7 D_{12}^g, \quad S_{13}^g = (a_7 + a_8) D_{13}^g, \quad S_{33}^g = \frac{1}{3} (2a_6 + 3a_7 + 4a_8) D_{33}^g.$$

In view of (3.12), the latter equations yield the following definitions for the material constants  $a_6$ ,  $a_7$  and  $a_8$ :

$$(3.16) \quad a_6 = 3\mu_{33} + \mu_{12} - 4\mu_{13}, \quad a_7 = 2\mu_{12}, \quad a_8 = 2(\mu_{13} - \mu_{12}).$$

Now let us introduce two dimensionless rheological parameters  $A$  and  $B$  that define the axial and prismatic shear viscosities in terms of the basal shear viscosity:

$$(3.17) \quad A = \frac{\mu_{33}}{\mu_{13}}, \quad B = \frac{\mu_{12}}{\mu_{13}},$$

and denote the viscosity  $\mu_{13}$  (the smallest viscosity among  $\mu_{33}$ ,  $\mu_{12}$  and  $\mu_{13}$ ) by  $\mu$ . With these definitions, the relations (3.16) become

$$(3.18) \quad a_6 = (3A + B - 4)\mu, \quad a_7 = 2B\mu, \quad a_8 = 2(1 - B)\mu,$$

where, for physical reasons,  $A \geq 1$ ,  $B \geq 1$ , and  $\mu > 0$ . In particular, when  $A = B = 1$ , then we deal with an isotropic grain, while the case  $A = B \rightarrow \infty$  (infinite axial and prismatic viscosities) corresponds to the situation in which the crystal can deform only by basal slip. On substituting (3.18) into (3.11), we obtain the frame-indifferent constitutive relation for the single crystal of ice given by

$$(3.19) \quad \mathbf{S} = 2\mu \left\{ \frac{1}{2} (3A + B - 4) \operatorname{tr}(\mathbf{MD}) \left( \mathbf{M} - \frac{1}{3} \mathbf{I} \right) + BD \right. \\ \left. + (1 - B) \left[ \mathbf{MD} + \mathbf{DM} - \frac{2}{3} \operatorname{tr}(\mathbf{MD}) \mathbf{I} \right] \right\}.$$

Using the Voigt notation (in which tensor components are expressed as elements of vectors), the flow law (3.19) can be re-written in the crystal co-ordinate system  $Ox_i^g$  in an alternative form as

$$(3.20) \quad \begin{pmatrix} S_{11}^g \\ S_{22}^g \\ S_{33}^g \\ S_{12}^g \\ S_{13}^g \\ S_{23}^g \end{pmatrix} = 2\mu \begin{pmatrix} \frac{1}{2}(A+B) & \frac{1}{2}(A-B) & & & & \\ \frac{1}{2}(A-B) & \frac{1}{2}(A+B) & & & & \\ & & A & & & \\ & & & B & & \\ & & & & 1 & \\ & & & & & 1 \end{pmatrix} \begin{pmatrix} D_{11}^g \\ D_{22}^g \\ D_{33}^g \\ D_{12}^g \\ D_{13}^g \\ D_{23}^g \end{pmatrix},$$

with the symmetric viscosity matrix depending on the three rheological parameters of the model: basal shear viscosity  $\mu$  and two dimensionless parameters  $A$  and  $B$  describing the degree of anisotropy of the single crystal. In a simplified model with  $A = B$ , the viscosity matrix takes a diagonal form, analogous to the form of the fluidity matrix considered by GAGLIARDINI and MEYSSONNIER [12], who used in their uniform stress model an inverse constitutive law for the crystal, in which the strain-rates are expressed in terms of the deviatoric stresses.

#### 4. Macroscopic behaviour of a polycrystal of ice

Assuming that each grain in the polycrystal has the same volume and the number of grains at a given material point does not change with time (as a result of recrystallisation, for instance), the components of any macroscopic tensor quantity are defined as an arithmetic mean of the corresponding components associated with all constituent grains

$$(4.1) \quad \bar{A}_{ij} = \frac{1}{N_g} \sum_{k=1}^{N_g} A_{ij}^{(k)},$$

where  $N_g$  is the number of crystals. According to ELVIN [10], the minimum number of grains required to obtain statistically satisfactory results of homogenisation should be at least 230.

The kinematic Eqs. (2.13) and (2.14) describing the evolution of the grain orientation, combined with the constitutive law for the grain given by (3.19), and supplemented by the averaging relation (4.1), do not suffice to describe completely the behaviour of the polycrystalline aggregate. For this reason, additional assumptions need to be introduced in order to provide further relations connecting the microscopic and macroscopic variables, required to close the system of equations.



In most of the models developed for ice (LLIBOUTRY [17], VAN DER VEEN and WHILLANS [32], GÖDERT and HUTTER [14], GAGLIARDINI and MEYSSONNIER [12], STAROSZCZYK [27]) it has been assumed that the stress state is uniform throughout the polycrystal, that is, at a given material point, the stress in each crystal equals that in the polycrystal. This assumption is known as the Sachs or Reuss approximation, and has been first introduced to ice mechanics by LLIBOUTRY [17], who has argued that the differences in the microstresses between adjacent ice crystals are negligibly small due to the process of continuous migration of crystal boundaries. In other branches of material science, however, for instance in metallurgy and structural geology, in common use are models, widely referred to as Taylor-Bishop-Hill (TBH) models, which are based on the assumption of the uniformity of deformation in the polycrystalline aggregate. Since both, Sachs-Reuss and Taylor, approaches do not account for the local interactions between constituent crystals, so they are both significant simplifications of the real intrinsic behaviour of the material, it seems that there is no obvious reason why one of the approaches should have much more advantage over the other. In fact, the results of numerical calculations carried out by MEYSSONNIER and PHILIP [22] by using the self-consistent model similar to that of CASTELNAU *et al.* [7], in which no assumptions on local stresses and strains are made, have demonstrated that the viscous response of isotropic polycrystalline ice aggregate given by the self-consistent approach is closer to that predicted by the Taylor model rather than the Sachs-Reuss model. In addition, which will be shown shortly, the Taylor approximation allows the theory to be correlated with the limit ice behaviour observed in simple experiments, whereas the analogous Sachs-Reuss model fails to do so (GAGLIARDINI and MEYSSONNIER [12], STAROSZCZYK [27]). It is also well known (BISHOP and HILL [4]) that the above two extreme approximations of the stress and the strain homogeneity in the polycrystal yield, respectively, lower and upper bounds for the stress at a given strain-rate. Therefore, it is of interest to develop for polycrystalline ice a model based on the deformation uniformity assumption to complement the afore-mentioned uniform stress models. Accordingly, in this work we adopt the Taylor (also known as the Voigt) assumption of the strain uniformity, which in terms of the velocity gradients takes the form:

$$(4.2) \quad \mathbf{L} = \bar{\mathbf{L}},$$

which necessarily implies that

$$(4.3) \quad \mathbf{D} = \bar{\mathbf{D}} \quad \text{and} \quad \mathbf{W} = \bar{\mathbf{W}}.$$

A consequence of the condition (4.2) is that, in general, the local stress  $\mathbf{S}$  is different in each crystal. This stress is defined by the constitutive law (3.19),

with the microscopic strain-rate  $\mathbf{D}$  now replaced by the macroscopic strain-rate  $\bar{\mathbf{D}}$ . The components of the macroscopic stress in the polycrystal  $\bar{\mathbf{S}}$  are then evaluated by applying the averaging relation (4.1), determining thus the relation between the macroscopic strain-rate and stress. In order to follow the evolution of the crystal orientation, described by Eqs. (2.13) and (2.14), we first apply the reciprocal of the relation (2.7) to find the strain-rate components expressed in the lattice frame  $Ox_i^g$  in terms of those measured in the global frame  $Ox_i$ , and then use the relations (4.3) to obtain:

$$(4.4) \quad D_{13}^g = \frac{1}{2} \sin 2\vartheta [\bar{D}_{11}(1 + \cos^2 \varphi) + \bar{D}_{22}(1 + \sin^2 \varphi) + \bar{D}_{12} \sin 2\varphi] \\ + \cos 2\vartheta (\bar{D}_{13} \cos \varphi + \bar{D}_{23} \sin \varphi),$$

$$(4.5) \quad D_{23}^g = \frac{1}{2} \sin \vartheta [(\bar{D}_{22} - \bar{D}_{11}) \sin 2\varphi + 2\bar{D}_{12} \cos 2\varphi] \\ - \cos \vartheta (\bar{D}_{13} \sin \varphi - \bar{D}_{23} \cos \varphi).$$

On substituting the above two relations into the kinematic Eqs. (2.13) and (2.14), with the spin tensor components  $W_{ij}$  replaced by  $\bar{W}_{ij}$ , we are able to calculate the angles  $\vartheta$  and  $\varphi$  defining the current orientation of the crystal  $c$ -axis.

Now determine the macroscopic viscosity of the isotropic polycrystalline ice,  $\mu_0$ , in terms of the single crystal rheological parameters  $\mu$ ,  $A$  and  $B$ . Supposing that the orientations of  $c$ -axes of all grains in the aggregate are uniformly distributed in space (an idealisation of the random fabric), and that the number of grains is sufficiently large, then each crystal (with its orientation defined by  $(\vartheta, \varphi)$ ) "occupies" the same elementary area  $\sin \vartheta d\vartheta d\varphi$  on a unit hemisphere of the radius  $r = 1$ . Hence, the number of grains on that hemisphere is  $N_g = 2\pi / \sin \vartheta d\vartheta d\varphi$ . With the number of grains increasing to infinity,  $N_g \rightarrow \infty$ , the summation in the relation (4.1) can be replaced by the surface integration, which, when applied to the deviatoric stress components, transforms the averaging formula into:

$$(4.6) \quad \bar{S}_{ij} = \frac{1}{2\pi} \int_0^{2\pi} \int_0^{\pi/2} S_{ij}(\vartheta, \varphi) \sin \vartheta d\vartheta d\varphi.$$

In order to establish the relation between the macroscopic and microscopic viscosities, consider a simple flow configuration, namely that of simple shear, in which the only non-zero strain-rate components are, say,  $\bar{D}_{13} = \bar{D}_{31}$ . For a grain



with the orientation given by  $(\vartheta, \varphi)$ , the crystal  $c$ -axis unit vector components in the global co-ordinate system are defined by  $\mathbf{c} = (\sin \vartheta \cos \varphi, \sin \vartheta \sin \varphi, \cos \vartheta)^T$ . The latter determines the structure tensor components  $M_{ij} = c_i c_j$ , which used in the constitutive law (3.19) yield the microscopic stress  $S_{13}$  as

$$(4.7) \quad S_{13} = 2\mu\bar{D}_{13} [(3A + B - 4) \sin^2 \vartheta \cos^2 \varphi \cos^2 \varphi + B + (1 - B)(\sin^2 \vartheta \cos^2 \varphi + \cos^2 \vartheta)].$$

After substituting the above equation into (4.6) and performing the prescribed integration, we find that the macroscopic stress  $\bar{S}_{13}$  is given by

$$(4.8) \quad \bar{S}_{13} = \frac{2}{5} \mu \bar{D}_{13} (A + 2B + 2),$$

which, by comparing to the viscous fluid flow law  $\bar{\mathbf{S}} = 2\mu_0 \bar{\mathbf{D}}$ , that is  $\bar{S}_{13} = 2\mu_0 \bar{D}_{13}$ , defines the macroscopic viscosity of the isotropic ice by

$$(4.9) \quad \mu_0 = \frac{\mu}{5} (A + 2B + 2).$$

From the above relation it follows that when the single crystal is isotropic (in which case  $A = B = 1$ ), then  $\mu_0 = \mu$ , implying that the microscopic and macroscopic viscous properties of ice are the same. On the other hand, when the single crystal is assumed to deform only by basal glide, which corresponds to  $A \rightarrow \infty$  and  $B \rightarrow \infty$ , then (4.9) gives an infinite value of the viscosity  $\mu_0$ , showing that in our model both the prismatic shear and axial deformations should be permitted in order to yield a bounded value of  $\mu_0$ . This result differs from the prediction of the uniform stress model, which allows the basal shear to be the only active slip system in the crystal, and yields for such a limit case of the grain anisotropy the relation  $\mu_0 = 2.5\mu$  (GAGLIARDINI and MEYSSONNIER [12], STAROSZCZYK [27]). In addition to (4.9), and using the results obtained in [27], we can express the ratio of the isotropic polycrystalline ice viscosities predicted by the Taylor and Sachs-Reuss theories, giving, respectively, the upper and lower bounds for  $\mu_0$ , as

$$(4.10) \quad \frac{\mu_0^T}{\mu_0^S} = \frac{1}{25} (A + 2B + 2)(A^{-1} + 2B^{-1} + 2),$$

where  $\mu_0^T$  and  $\mu_0^S$  denote, respectively, the viscosities predicted by the Taylor and Sachs-Reuss approximations. Obviously,  $\mu_0^T/\mu_0^S = 1$  for  $A = B = 1$ , defining isotropic grains.

As the polycrystal deforms under uniaxial compression or simple shear (which will be illustrated in the next section), the crystals gradually rotate in such a way

that, ultimately, all the  $c$ -axes are aligned in parallel. In such a limit situation, the macroscopic properties of the aggregate become those of the single crystal, with the material behaviour described by the constitutive Eqs. (3.19) and (3.20). Hence, using (3.17) and (4.9), the relation (3.20) yields the limit macroscopic viscosity for shearing in planes parallel to the crystal  $c$ -axes in the form:

$$(4.11) \quad \frac{\mu_{13}}{\mu_0} = \frac{5}{A + 2B + 2}.$$

Similarly, the limit macroscopic viscosities for shear in the plane normal to the crystal  $c$ -axes (prismatic shearing), for uniaxial compression along the  $c$ -axes, and for uniaxial compression in the direction normal to the  $c$ -axes, are given, respectively, by

$$(4.12) \quad \frac{\mu_{12}}{\mu_0} = \frac{5B}{A + 2B + 2}, \quad \frac{\mu_{33}}{\mu_0} = \frac{5A}{A + 2B + 2}, \quad \frac{\mu_{11}}{\mu_0} = \frac{5(A + 3B)}{4(A + 2B + 2)}.$$

In laboratory tests carried out on samples of polycrystalline ice, usually only the viscosities for simple shear and unconfined uniaxial compression are measured. The reciprocals of the limit ratios of these viscosities to the isotropic viscosity for indefinite deformations, that is  $\mu_0/\mu_{13}$  and  $\mu_0/\mu_{33}$ , are commonly described in glaciology as enhancement factors for shear and compression,  $E_s$  and  $E_a$ , respectively (BUDD and JACKA [6]). By substituting the experimentally measured values of the enhancement factors to Eqs. (4.11) and (4.12)<sub>2</sub>, we can determine the values of the two rheological parameters  $A$  and  $B$  in our model. As a result, we obtain the following relations for  $A$  and  $B$ :

$$(4.13) \quad A = \frac{E_s}{E_a}, \quad B = \frac{5E_s}{2} - \frac{E_s}{2E_a} - 1,$$

which ensure the correlation between the observed limit behaviour of polycrystalline ice and the model predictions.

## 5. Numerical simulations

The model formulated in the previous sections is now applied to simulate the viscous behaviour of polycrystalline ice in two simple configurations, corresponding to those occurring in typical laboratory tests, namely the unconfined uniaxial compression and simple shear. As first, we determine the microscopic rheological parameters  $A$  and  $B$ , related by Eq. (4.13) to the macroscopic enhancement factors. BUDD and JACKA [6] have measured in tests conducted on warm ice (near melting) the enhancement factors  $E_a = 3$  and  $E_s = 8$ , whose meaning is that both axial and shear viscosities decrease with increasing deformation of ice.



However, as the data presented by PIMIANTA *et al.* [25] and THORSTEINSSON *et al.* [31] indicate, the axial viscosity of polar ice increases with deformation, hence  $E_a < 1$  seems more appropriate, especially at low temperatures and low stress levels characteristic of natural ice masses. The value of  $E_a$  as small as 1/10 for a single-maximum fabric has been found experimentally by PIMIANTA *et al.* [25], although recently MANGENEY *et al.* [19] have suggested the value  $E_a \sim 1/3$  for ice near the bottom of the Greenland ice cap, calculated by applying the constitutive model developed by LLIBOUTRY [17] and the field data provided by THORSTEINSSON *et al.* [31]. The shear enhancement factor for ice near the centre of the Greenland ice sheet has been evaluated to be  $E_s \approx 2.5$ , though it seems that further away from the centre, where shear stresses are larger (and hence fabrics are stronger), a higher value is more relevant. Accordingly, in our simulations we adopt the enhancement factors  $E_a = 1/3$  and  $E_s = 5$ , for which the relations (4.13) give  $A = 15$  and  $B = 4$ . It should be noted here that it is not possible to achieve the above enhancement factors by employing uniform stress models (GÖDERT and HUTTER [14], GAGLIARDINI and MEYSSONNIER [12]), with a single parameter describing the crystal anisotropy, in which case the maximum value of  $E_s$  that can be attained is 2.5.

Assume that the uniaxial compression is carried out along the  $x_3$  direction, with equal strains in both lateral directions  $x_1$  and  $x_2$ . Then the deformation field is described by

$$(5.1) \quad x_1 = \lambda_1 X_1, \quad x_2 = \lambda_2 X_2, \quad x_3 = \lambda_3 X_3, \quad \lambda_1 = \lambda_2 = \lambda_3^{-1/2},$$

where  $\lambda_i$  ( $i = 1, 2, 3$ ) are the principal stretches along the  $x_i$  axes, all equal to unity at the start of flow from the isotropic state and  $\lambda_3 < 1$  afterwards, and the last relation in (5.1) is due to the ice incompressibility condition  $\lambda_1 \lambda_2 \lambda_3 = 1$ . The velocities are defined by

$$(5.2) \quad v_1 = -\frac{1}{2} x_1 \dot{\lambda}_3 / \lambda_3, \quad v_2 = -\frac{1}{2} x_2 \dot{\lambda}_3 / \lambda_3, \quad v_3 = x_3 \dot{\lambda}_3 / \lambda_3,$$

so the tensors of macroscopic velocity gradient  $\bar{\mathbf{L}}$ , strain-rate  $\bar{\mathbf{D}}$ , and spin  $\bar{\mathbf{W}}$  are given by

$$(5.3) \quad \bar{\mathbf{L}} = \bar{\mathbf{D}} = \begin{pmatrix} -\frac{1}{2} \dot{\lambda}_3 / \lambda_3 & 0 & 0 \\ 0 & -\frac{1}{2} \dot{\lambda}_3 / \lambda_3 & 0 \\ 0 & 0 & \dot{\lambda}_3 / \lambda_3 \end{pmatrix}, \quad \bar{\mathbf{W}} = \mathbf{0}.$$

In the calculations, performed for the isotropic ice viscosity  $\mu_0 = 10 \text{ MPa a}$ , where the unit "a" stands for a year, it has been assumed that the axial strain

rate  $\bar{D}_{33} = \dot{\lambda}_3/\lambda_3 = 10^{-3} \text{ a}^{-1}$  is kept constant throughout the flow. All the simulations have been carried out with  $N_g = 800$  discrete grains whose initial orientations have been distributed at random. In the plots, the axial deformation along the  $x_3$ -axis is expressed in terms of the axial strain  $\varepsilon_{33}$  defined by

$$(5.4) \quad \varepsilon_{33} = \lambda_3 - 1.$$

The evolution of ice fabric with the axial deformation  $\varepsilon_{33}$  is illustrated by means of the equal-area Schmid diagrams shown in Fig. 2, in which the dots represent the positions at which the individual crystal  $c$ -axes intersect the unit hemisphere, projected onto the plane of the plot. The diagrams demonstrate how the single grains rotate and gradually align in the direction of the principal axis of compression, which for large deformations gives rise to a single-maximum fabric, with nearly all  $c$ -axes clustered around the  $x_3$ -axis. Such a behaviour of polycrystalline ice aggregate, predicted by the model, agrees well with the behaviour observed in both the laboratory conditions and in the field (PIMIENIA *et al.* [25], BUDD and JACKA [6], ALLEY [1], THORSTEINSSON *et al.* [31]).

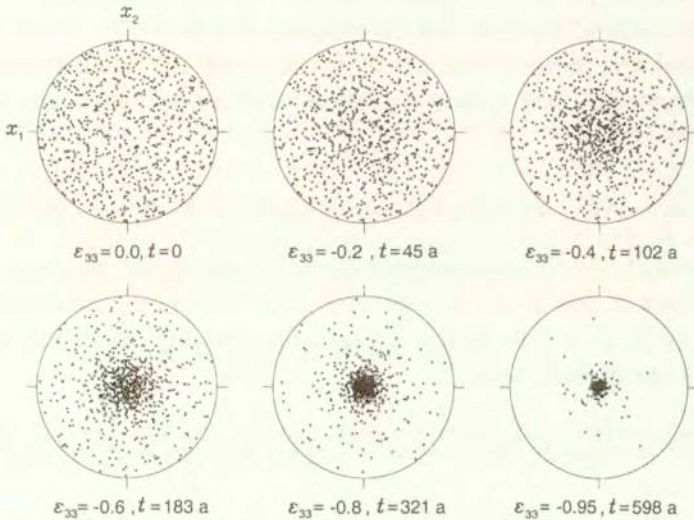


FIG. 2. Evolution of fabric in uniaxial compression along the  $x_3$ -axis as a function of the macroscopic axial strain  $\varepsilon_{33}$  and time  $t$  (in years).

Figure 3 illustrates the evolution of the macroscopic axial viscosity with increasing compressive strain as a function of the crystal rheological parameters  $A$  and  $B$ . The axial viscosity is defined in terms of the current macroscopic stress  $\bar{S}_{33}$  and the prescribed strain-rate  $\bar{D}_{33}$  by the relation  $\mu_{33} = \bar{S}_{33}/(2\bar{D}_{33})$ , and is normalised by the macroscopic viscosity  $\mu_0$ , that is the ratios  $\mu_{33}/\mu_0$  are plotted in the figure.



Figure 4 shows the variation of the normalised macroscopic viscosities  $\mu_{ij}/\mu_0^T$  (solid lines) with the strain  $\epsilon_{33}$  for the single crystal rheological parameters  $A = 15$  and  $B = 4$ , demonstrating the evolution of the strength of anisotropy (in this case transverse isotropy) of the aggregate with increasing macroscopic deformation. For comparison, also the results predicted by the related uniform stress model by STAROSZCZYK [27], indicated by the dashed lines, are presented

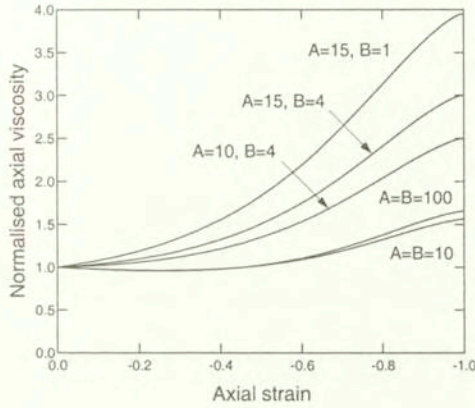


FIG. 3. Evolution of the normalised axial viscosity with the strain  $\epsilon_{33}$  in uniaxial compression for different values of the crystal rheological parameters  $A$  and  $B$ .

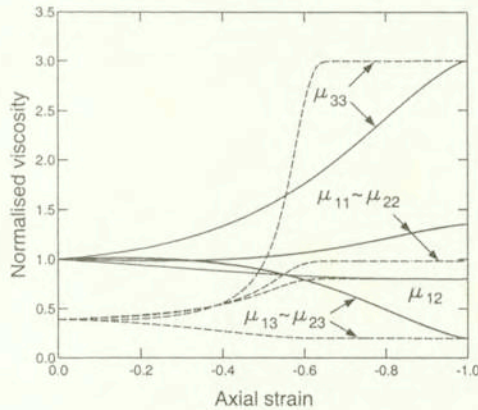


FIG. 4. Evolution of the normalised viscosities with the strain  $\epsilon_{33}$  in uniaxial compression for the crystal rheological parameters  $A = 15$  and  $B = 4$ . Comparison of uniform strain (—) and uniform stress (---) model results.

in the figure. We note that (1) the isotropic ice viscosities (occurring at  $\epsilon_{33} = 0$ ) predicted by the uniform strain and uniform stress models, are, for the chosen

single crystal parameters, in the ratio  $\mu_0^T/\mu_0^S = 2.5667$  determined by (4.10), and (2) the same limit viscosities  $\mu_{11}$ ,  $\mu_{12}$  and  $\mu_{13}$  when  $\varepsilon_{33} \rightarrow -1$ , for the Taylor model given by (4.11) and (4.12), are predicted by the two theories. However, it is seen that the limit viscosities given by the two models are approached in different ways. For the uniform stress model, the most significant evolution in the fabric strength occurs for the axial strains  $\varepsilon_{33}$  changing from  $-0.4$  to  $-0.6$ , with the limit values reached just after the latter value is exceeded, while for the uniform strain model, which predicts a "stiffer" behaviour of ice, the limit alignment of individual grains, and hence the limit viscosities, are attained much later, at  $\varepsilon_{33}$  close to  $-1$ .

Next consider a simple shear in the plane  $Ox_1x_3$  started from an initially isotropic state. The deformation field is now described by

$$(5.5) \quad x_1 = X_1 + \kappa X_3, \quad x_2 = X_2, \quad x_3 = X_3,$$

where  $\kappa$  is a shear strain increasing from zero. The associated velocity field is given by

$$(5.6) \quad v_1 = \dot{\kappa}x_3, \quad v_2 = v_3 = 0,$$

yielding the macroscopic velocity gradient, strain-rate, and spin tensors of the forms:

$$(5.7) \quad \bar{\mathbf{L}} = \begin{pmatrix} 0 & 0 & \dot{\kappa} \\ 0 & 0 & 0 \\ 0 & 0 & 0 \end{pmatrix}, \quad \bar{\mathbf{D}} = \begin{pmatrix} 0 & 0 & \frac{1}{2}\dot{\kappa} \\ 0 & 0 & 0 \\ \frac{1}{2}\dot{\kappa} & 0 & 0 \end{pmatrix}, \quad \bar{\mathbf{W}} = \begin{pmatrix} 0 & 0 & \frac{1}{2}\dot{\kappa} \\ 0 & 0 & 0 \\ -\frac{1}{2}\dot{\kappa} & 0 & 0 \end{pmatrix}.$$

The process of formation and subsequent development of fabric during simple shear is illustrated in Fig. 5. We note that in this flow regime the crystals initially rotate towards the plane  $Ox_2x_3$ , and only at very large shear strains  $\kappa$  their  $c$ -axes cluster around the axis  $x_3$  (which becomes the principal axis of compression as  $\kappa \rightarrow \infty$ ). Ultimately, the same single-maximum fabric as in the uniaxial compression develops.

The evolution of the macroscopic viscosities during simple shear deformation is illustrated in Fig. 6 and 7. A characteristic feature that is seen in the figures is an initial hardening (an increase in the shear viscosity  $\mu_{13}$ ) of ice under shearing, with a maximum shear viscosity occurring at the strains  $\kappa \sim 2$ . Figure 6 shows the dependence of the normalised viscosity  $\mu_{13}/\mu_0$  of the aggregate on the parameters  $A$  and  $B$  describing the anisotropy of constituent crystals. It can be observed that now, compared to uniaxial compression (see Fig. 3), the macroscopic behaviour of the polycrystal is less sensitive to particular values



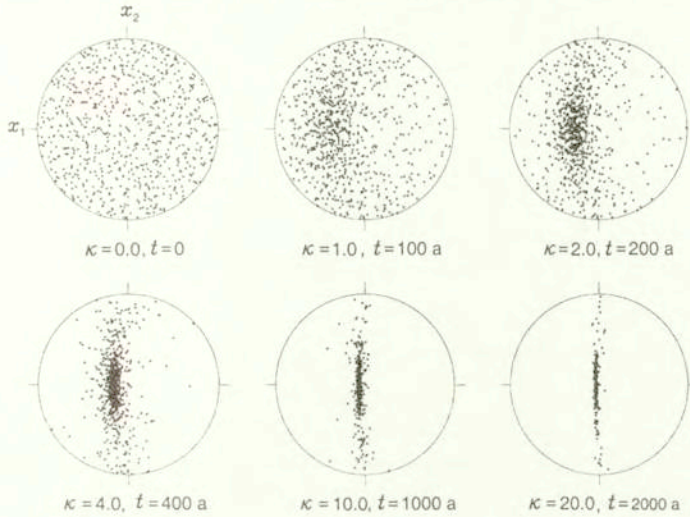


FIG. 5. Evolution of fabric in simple shear in the  $Ox_1x_3$  plane as a function of the macroscopic shear strain  $\kappa$  and time  $t$  (in years).

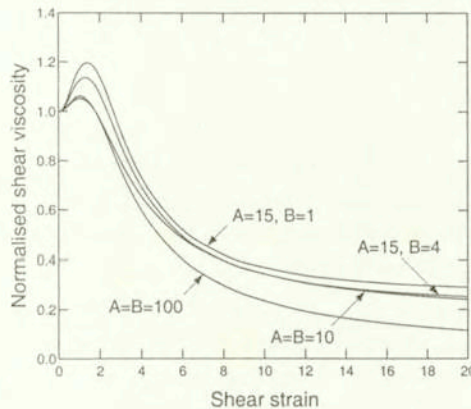


FIG. 6. Evolution of the normalised shear viscosity with the strain  $\kappa$  in simple shear for different values of the crystal rheological parameters  $A$  and  $B$ .

of the microscopic rheological parameters. Figure 7 demonstrates, for  $A = 15$  and  $B = 4$ , the evolution of the instantaneous viscosities  $\mu_{ij}/\mu_0$  with increasing shear strain  $\kappa$ , showing the development of anisotropy from the initially isotropic fabric at  $\kappa = 0$ . Since the fabric at the limit  $\kappa \rightarrow \infty$  coincides with that created at large deformations during uniaxial compression, the full anisotropy gradually transforms into transverse isotropy, with  $\mu_{13} \rightarrow \mu_{23}$  and  $\mu_{11} \rightarrow \mu_{22}$ . Moreover, the limit viscosities plotted in Fig. 7, as being again described by the

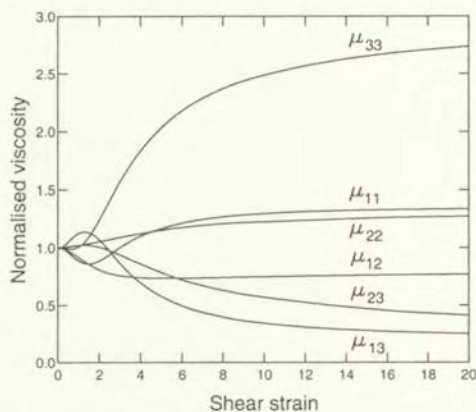


FIG. 7. Evolution of the normalised viscosities with the strain  $\kappa$  in simple shear for the crystal rheological parameters  $A = 15$  and  $B = 4$ .

relations (4.11) and (4.12), are equal to the limit viscosities shown in Fig. 4:  $\mu_{13}/\mu_0 = 0.2 = 1/E_s$ ,  $\mu_{33}/\mu_0 = 3.0 = 1/E_a$ ,  $\mu_{12}/\mu_0 = 0.8$ , and  $\mu_{11}/\mu_0 = 1.35$ .

## 6. Conclusions

The process of induced anisotropy in polycrystalline ice has been modelled by assuming that an individual crystal of ice is a transversely isotropic material, and that the strain is uniform throughout the polycrystal. The creep behaviour of the single crystal has been described by two parameters defining the strength of its anisotropy. The magnitudes of these parameters have been correlated with the limit viscosities in compression and simple shear observed in experiments, something which is not possible with the analogous uniform stress models. Although the viscous response of the single crystal has been assumed to be a linear relation connecting the deviatoric stress to strain-rate, non-linearity of the material behaviour can be easily accounted for by relating the viscosity of ice to a function of the strain-rate invariant  $\text{tr } \mathbf{D}^2$ , which is a well established approach in theoretical glaciology. In the proposed model only the crystal lattice rotation mechanism has been considered, and the effects of the rotation and dynamic recrystallisation on the fabric development in polycrystalline ice have not been taken into account. The reason for not including the latter mechanisms into the model is an insufficient amount of experimental data enabling the proper identification of the main factors controlling such complex microprocesses. Once these factors are identified and quantified, then the present model can be applied as a framework for incorporating more features of the creep behaviour of ice.



## References

1. R. B. ALLEY, *Flow-law hypotheses for ice-sheet modelling*, J. Glaciol., **38**, 129, 245–256, 1992.
2. N. AZUMA, *A flow law for anisotropic ice and its application to ice sheets*, Earth Planet. Sci. Lett., **128**, 3–4, 601–614, 1994.
3. D. R. BARAL, K. HUTTER and R. GREVE, *Asymptotic theories of large-scale motion, temperature, and moisture distribution in land-based polythermal ice sheets: A critical review and new developments*, Appl. Mech. Rev., **54**, 3, 215–256, 2001.
4. J. F. W. BISHOP and R. HILL, *A theory of plastic distortion of a polycrystalline aggregate under combined stresses*, Phil. Mag. (7<sup>th</sup> Ser.), **42**, 327, 414–427, 1951.
5. J. P. BOEHLER, *Representations for isotropic and anisotropic non-polynomial tensor functions*, [in:], Applications of Tensor Functions in Solid Mechanics, J. P. BOEHLER [Ed.], pp. 31–53, Springer, Wien 1987.
6. W. F. BUDD and T. H. JACKA, *A review of ice rheology for ice sheet modelling*, Cold Reg. Sci. Technol., **16**, 2, 107–144, 1989.
7. O. CASTELNAU, P. DUVAL, R. A. LEBENSOHN and G. R. CANOVA, *Viscoplastic modeling of texture development in polycrystalline ice with a self-consistent approach: Comparison with bound estimates*, J. Geophys. Res., **101**, B6, 13851–13868, 1996.
8. C. S. M. DOAKE and E. W. WOLFF, *Flow law for ice in polar ice sheets*, Nature, **314**, 6008, 255–257, 1985.
9. P. DUVAL, M. F. ASHBY and I. ANDERMAN, *Rate-controlling processes in the creep of polycrystalline ice*, J. Phys. Chem., **87**, 21, 4066–4074, 1983.
10. A. A. ELVIN, *Number of grains required to homogenize elastic properties of polycrystalline ice*, Mech. Mat., **22**, 1, 51–64, 1996.
11. O. GAGLIARDINI, M. ARMINJON and D. IMBAULT, *An inhomogeneous variational model applied to predict the behaviour of isotropic polycrystalline ice*, Arch. Mech., **53**, 1, 3–21, 2001.
12. O. GAGLIARDINI and J. MEYSSONNIER, *Analytical derivations for the behavior and fabric evolution of a linear orthotropic ice polycrystal*, J. Geophys. Res., **104**, B8, 17797–17809, 1999.
13. J. W. GLEN, *The creep of polycrystalline ice*, Proc. R. Soc. Lond., A **228**, 1175, 519–538, 1955.
14. G. GÖDERT and K. HUTTER, *Induced anisotropy in large ice shields: Theory and its homogenization*, Continuum Mech. Thermodyn., **10**, 5, 293–318, 1998.
15. J. W. HUTCHINSON, *Bounds and self-consistent estimates for creep of polycrystalline materials*, Proc. R. Soc. Lond., A **348**, 1652, 101–127, 1976.
16. W. B. KAMB, *The glide direction in ice*, J. Glaciol., **3**, 30, 1097–1106, 1961.
17. L. LLIBOUTRY, *Anisotropic, transversely isotropic nonlinear viscosity of rock ice and rheological parameters inferred from homogenization*, Int. J. Plast., **9**, 5, 619–632, 1993.
18. L. LLIBOUTRY and P. DUVAL, *Various isotropic and anisotropic ices found in glaciers and polar ice caps and their corresponding rheologies*, Ann. Geophys., **3**, 2, 207–224, 1985.

19. A. MANGENEY, F. CALIFANO and O. CASTELNAU, *Isothermal flow of an anisotropic ice sheet in the vicinity of an ice divide*, J. Geophys. Res., **101**, B12, 28189–28204, 1996.
20. A. MANGENEY, F. CALIFANO and K. HUTTER, *A numerical study of anisotropic, low Reynolds number, free surface flow for ice sheet modeling*, J. Geophys. Res., **102**, B10, 22749–22764, 1997.
21. J. MEYSSONNIER and A. PHILIP, *A model for tangent viscous behaviour of anisotropic polar ice*, Ann. Glaciol., **23**, 253–261, 1996.
22. J. MEYSSONNIER and A. PHILIP, *Remarks on self-consistent modelling of polycrystalline ice*, [in:] K. HUTTER, Y. WANG and H. BEER [Eds.], *Advances in Cold-Region Thermal Engineering and Sciences*, pp. 225–236, Springer, Berlin 1999.
23. A. MOLINARI, G. R. CANOVA and S. AHZY, *A self-consistent approach of the large deformation polycrystal viscoplasticity*, Acta Metall., **35**, 12, 2983–2994, 1987.
24. L. W. MORLAND and R. STAROSZCZYK, *Viscous response of polar ice with evolving fabric*, Continuum Mech. Thermodyn., **10**, 3, 135–152, 1998.
25. P. PIMIENTA, P. DUVAL and V. Y. LIPENKOV, *Mechanical behavior of anisotropic polar ice*, [in:] International Association of Hydrological Sciences Publication no. 170, pp. 57–66, 1987, (Symp. Physical Basis of Ice Sheet Modelling, Vancouver 1987).
26. R. STAROSZCZYK, *An orthotropic constitutive model for secondary creep of ice*, Arch. Mech., **53**, 1, 65–85, 2001.
27. R. STAROSZCZYK, *A uniform stress, discrete-grain model for induced anisotropy of ice*, [in:] Applications of Mechanics in Civil and Hydro-Engineering, K. SZMIDT [Eds.], pp. 295–314, IBW PAN Publishing House, Gdańsk 2001.
28. R. STAROSZCZYK and L. W. MORLAND, *Orthotropic viscous response of polar ice*, J. Eng. Math., **37**, 1-3, 191–209, 2000.
29. R. STAROSZCZYK and L. W. MORLAND, *Plane ice-sheet flow with evolving orthotropic fabric*, Ann. Glaciol., **30**, 93–101, 2000.
30. B. SVENDSEN and K. HUTTER, *A continuum approach for modelling induced anisotropy in glaciers and ice sheets*, Ann. Glaciol., **23**, 262–269, 1996.
31. T. THORSTEINSSON, J. KIPFSTUHL and H. MILLER, *Textures and fabrics in the GRIP ice core*, J. Geophys. Res., **102**, C12, 26583–26599, 1997.
32. C. J. VAN DER VEEN and I. M. WHILLANS, *Development of fabric in ice*, Cold Reg. Sci. Technol., **22**, 2, 171–195, 1994.

Received July 31, 2001; revised version December 3, 2001.